Available online at www.ijtnbm.ir

The Iranian Journal of Textile Nano-bio Modificatior

IJTNBM 1 (2022) 27–47

Development and Characterization of Graphene Oxide based Composite for Adsorptive Removal of Azo Reactive Dyes from Aqueous Media

Zahra Zareei[a*], Mohammadali Shirgholami[a], Saeid Jafari[a], Mohammad Dehghani Ahmadabadi[a], Masoud Rohani-moghadam[b]

[a]*Department of polymer engineering, Yazd branch, Islamic Azad University, Yazd, Iran*
[b]*Department of Chemistry, Faculty of Sciences, Vali-e-Asr University of Rafsanjan, Rafsanjan, Iran*

Received 2 February 2022; revised 20 June 2022; accepted 25 June 2022

Abstract

In this study, we tried to present an efficient method for removal of Reactive red 241 (RR241) from aqueous media, using a modified carbon composite with GO sheets. The prepared nanocomposites were then characterized by commonly identical techniques involving FESEM, BET, and FT-IR. In removal studies, various parameters affecting the adsorption process including pH, time, adsorbent dose, temperature as well as the amount of GO in the construction of composite were studied by response surface method. The optimum conditions for 100 mg/L dye removal was pH of 5.0, 75 minutes' time, and the adsorbent dose of 1.47 g/L containing 4.15 wt.% of GO. Also, under optimum conditions, the maximum, 96% removal, was achieved. Experiments showed that the adsorption was more consistent with the Langmuir equations, and the maximum adsorption under this model was 160 mg/g. The removal experiments showed that the amount of the adsorbent, GO content and pH had a significant effect on RR241 removal. BET analysis indicated that the addition of GO to the carbon composite structure improved the pore size, total pore volume, and effective surface area of the composite. Also, isotherms, kinetics, and thermodynamic studies of adsorption depicted that the Langmuir isotherm model, pseudo-second-order kinetic model, and self-adsorption are suitable models for RR241dye adsorption.

Keywords: Colorful Pollutants, Adsorption, Graphene Oxide, Composite.

[*]* Corresponding author. Tel: +98-353187822
E-mail address: z.zareei@iauyazd.ac.ir

1. Introduction

In today's world, color plays a vital role in cultivating human tastes and satisfying their aesthetic needs [1]. The use of dye in textile and decorative goods has been common since ancient times due to its beauty and effect on the human soul [2]. Many advances have been made in the field of dyeing and production of dyes for a long time. Today this industry has been able to offer the most desirable dyed goods to the market in various shades by using the latest dyeing techniques and different types of dyes [3]. In the dyeing process, four factors play major roles: dyes, goods, auxiliary chemicals, and machines [4]. Dyes used in the dyeing process are classified in two ways, one is based on chemical structure, and the other based on the type of application. In chemical class, dyes are classified into pigments, acidic dyes, azo dyes, anthraquinone dyes, vat dyes, indigo dyes, triaryl carbonium dyes, polymethine dyes, metallic dyes, Nitro and nitroso dyes and miscellaneous dyes [5]. Azo dyes are a group of reactive dyes that make up about 70-60% of all dyes used in various industries. These dyes are generally covalently bonded with textile fibers such as cotton. Due to their low degradability and widespread use, they have influenced conventional wastewater treatment in the textile industry in recent decades [6]. Today, the discharge of effluents from textile industries into natural waters has created serious problems. These color compounds are toxic to aquatic life [7]. They are visible in amounts less than one milligram per liter and cause unpleasant environmental scenery. It has also been shown that some azo dyes or compounds resulting from the degradation of color compounds are toxic, mutagenic, carcinogenic, and contain resistant compounds [8]. Therefore, it is very necessary for textile industries to have wastewater treatment before discharging effluents to the environment. Treatment of colored wastewater is relatively difficult by conventional biological and physicochemical processes due to the structure of the chemical complex of these dyes, especially azo dyes [9].

So far, various methods such as ion exchange [10], chemical precipitation [11], reverse osmosis [12], membrane technologies [13], coagulation [14], electrochemical purification [15], which have problems such as the need for continuous recovery, preliminary treatment, extremely high cost, biological sludge, and strict operating conditions. Coagulation, photolysis, and advanced oxidation are among the methods which have some disadvantages. High cost and time-consuming, low efficiency, high energy consumption and the need for reactive materials are some disadvantages of these methods. Among the various available methods, adsorption is one of the most effective processes for the removal that is both environmentally friendly and easy to operate [16]. The adsorption process has been suggested as an extensible process due to the low cost of design and operation, non-production of hazardous byproducts and the design simplicity to remove organic and inorganic compounds [17-18]. Over recent years, applications of graphene oxide (GO) in various fields have attracted the attention of scientists. GO is one of the graphene derivatives widely used as a potential superior adsorbent. Its excellent properties and the ability to control its properties through chemical functionalization have caused researchers to pay particular attention to it [19-20]. GO is a layer of graphite with numerous groups containing oxygen. GO, as a two-dimensional carbon allotrope has a lattice-like planar structure [21]. GO shows strange physical properties that have never been observed before at the nanoscale. High Young's modulus (about 1000 GPa), high fracture resistance (130 GPa), good heat conductivity (5000 W/mK), special surface area (2600 m2g-1), and amazing transfer phenomena such as the quantum Hall effect, the ability to absorb some metal ions and soil pollutants, and the catalytic properties are remarkable properties of GO [22]. A large number of oxygen-containing groups, such as epoxy, hydroxyl, and carboxyl groups at the plane structure of GO can be bonded with metal ions. In addition, the high surface of GO gives it a high adsorption capacity similar to that of carbon nanotubes [23]. The main limitation of the application of the GO is its separation from the solution after the adsorption process and the turbidity of the material in the sample [24]. Therefore, creating conditions for separation, optimum use of graphene, and transparent effluent production is an inevitable necessity. To overcome this limitation, several researchers have suggested modifying or merging it with other materials. Bhattacharyya et al. prepared a nanocomposite consisting of activated carbon graphene oxide as the adsorbent of methylene blue dye from the solution [25]. Martins et al. proposed a mixture of high superficial area carbon-

based nanomaterial strategy to improve the removal of basic blue 26 (BB26) by blending porous carbon nitride (CN) and graphene oxide (GO). The CN/GO nanocomposite's ability to remove the BB26 dye was 21 times higher than those reported in the literature, indicating CN/GO composites as potential filtering materials for basic dyes [26]. In another study, Cao et al. reported a novel GO/PNIPAM composite system that had been rationally designed for the removal of organic dyes from polluted water in a new mechanism- an extraction-like mechanism. The system gives a phase transition to produce a solution phase and a gel phase at temperatures above the lower critical solution temperature (LCST) of PNIPAM. During this phase the GO sheets are fully transferred into the gel phase. [27]. Rostamian et al. have proposed an eco-friendly adsorbent based on poly (glycerol sebacate) (PGS), including PGS-graphene oxide nanoparticles (GO), PGS-graft-chitosan(CS), and PGS–CS–GO nanocomposites as efficient dye adsorbents for the wastewater treatment procedure [28].

This study aimed at of this study was to synthesizing a GO-based carbon composite (GO-CC) as a suitable and environmentally friendly adsorbent for the removal of Reactive red 241 (RR241) dye from aqueous solutions. The effect of various variables such as solution pH, contact time, amount of GO on carbon composite, and amount of carbon composite as adsorbent on removal efficiency was investigated. Statistical modeling and optimization of removal conditions were performed using response surface methodology (RSM). The reason for using statistical modeling of RSM were benefits such as simplicity, reduction in the number of samples tested, comprehensive study of the simultaneous effect of variables on response, reduction of time, manpower, and cost. In addition, the kinetic and equilibrium data of adsorption with pseudo-first and pseudo-second kinetic models and Freundlich and Langmuir isotherm models were investigated.

2. Experimental

2.1. Chemicals

GO powder (Sigma-Aldrich, USA) and graphite powder (Merck, Germany) were used to prepare the carbon composite. The carbon composite was fabricated via sol gel using potassium trimethoxy silane (90% purity, Merck), methanol (99% purity, Merck), and hydrochloric acid (37% aqueous solution, Sigma-Aldrich). The removal experiments were performed on Reactive red 241 (RR 241,98% purity, Sigma-Aldrich) in a batch reactor. Its chemical structure is illustrated in Scheme 1.

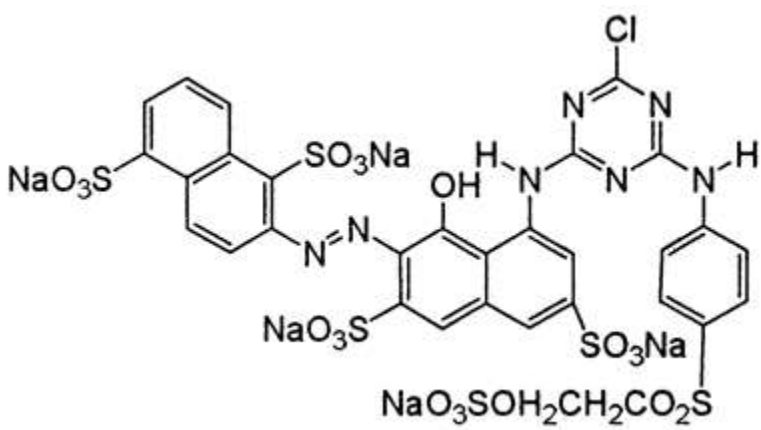

Scheme 1- Chemical structure of Reactive Red 241.

The pH of the aqueous solutions was adjusted using a 0.1 M phosphate buffer consisting of phosphoric acid (85% purity, Sigma-Aldrich) and sodium hydroxide (purity of 98%, Sigma-Aldrich), and an Autolab model 827

pH meter was used to measure it. A Fartest magnetic stirrer (Model HPMA 700, Farzaneh Arman Ltd.) was used to disperse the adsorbent in aqueous solutions during the test. The carbon nanocomposites were separated from aqueous samples by an Eppendorf 5810 Centrifuge device (MiniSpin, Germany). The concentration of RR241 in aqueous solutions was determined using the Cary 100 UV-Vis spectrophotometers (Agilent USA).

2.2. Preparation of the adsorbent

The adsorbent used to remove the RR241 from aqueous solutions was a carbon-composite, which contained GO platelets, prepared by sol-gel method at ambient temperature. The fabrication way for this composite is derived from Esfandiary et al., which is briefly described below. To prepare the sol (4 mL), first 3 mL of methanol was mixed with 600 µL of deionized water, and then 100 µL of potassium trimethoxy silane was added to the mixture. The gelation process of the resulting mixture (siloxane condensation polymerization) began with the reduction of the solution pH to the range of 5.0-6.0. The process was accelerated by the addition of a few drops of hydrochloric acid. After the formation of three-dimensional polymer gels containing repeating SiO2 units, the sol color changed from transparent to milky.In the next step, 41.0 mg of GO powder was mixed with 1.0 g of graphite powder. Then, the sol-gel mixture prepared in the previous step was added to the carbon mass and gently homogenized with the spatula to produce a carbon paste. The resulting carbon paste was placed in a preheated oven at 60 °C for one hour. The composite powder was kept in desiccator until its subsequent usage in the adsorption experiments.

2.3. Adsorption tests

RR241 adsorption experiments were conducted in a batch reactor to investigate the effect of various variables such as the weight percentage of GO in the prepared composite, solution pH, the adsorbent dosage (i.e. amount of the composite) and reaction time on the dye removal efficiency using the GO-modified carbon composite by the models presented in Design of Expert (DOE) software. In the optimum conditions, 147 mg of the adsorbent containing 4.15 wt. % of GO was added to 100 mL of the buffer phosphate (0.1 M) containing 100 mg/L of RR241 with the pH of 5.0 for 75 min. After completion of the planned adsorption time, the composite was separated from the aqueous solution by centrifugation and the residual concentration of RR241 in the solution was measured using the uv-vis spectrophotometer. Finally, the dye removal efficiency (Re (%)) and the adsorbent adsorption capacity (qe) were calculated using Equations 1 and 2, respectively.

$$Re\ (\%) = \frac{C_0 - C_e}{C_0} \times 100 \qquad \text{(Eq. 1)}$$

$$q = \frac{(C_0 - C_e)v}{m} \qquad \text{(Eq. 2)}$$

In these equations, C0 and Ce are initial and final concentrations of RR241 in mg/L, respectively, and V and m are solution volume (L) and the adsorbent absorbed mass in grams, respectively.

2.4. Determination of isoelectric point of the prepared composite

The pH of the isoelectric point of the prepared carbon composite was estimated by adding 1.0 g of GO-modified carbon composite to bottles containing 50 mL of 0.1 M potassium nitrate, the pH of which was adjusted at a certain value in the range of 2.0–12.0 using the hydrochloric acid and sodium hydroxide. The mixture was agitated by the magnetic stirrer for 48 h. Then, the final pH of the solution was measured using an 827 Autolab pH meter. The final pH was plotted against the initial pH and a line was also drawn where final pH = initial pH. The intersection point of the final pH-initial pH curve and a line where pH= initial pH was introduced as the pH of the isoelectric point.

2.5. Design of the studies and optimization of dye removal

This study investigated the effect of pH, adsorption time, amount of GO used for fabrication of the carbon composite and amount of the carbon composite used for the RR241 removal, using Design of Expert (DOE) software. Sample size and a number of tests were calculated by response surface method (RSM) using central composite design (CCD). The efficiency of the dye removal was selected as the response in the design of experiments, as shown in Table 1.

Table 1 Experimental range and levels of the independent variables

Parameters	**Unit**	**Symbol**	**Levels**				
			α-	-1	0	1	α
pH	-	X_1	2	4.25	6.5	8.75	11
Time	min	X_2	20	45	70	95	120
GO content	Wt. %	X_3	0.1	1.325	2.55	3.775	5
Adsorbent (GO-CC)	g/L	X_4	0. 1	0.575	1.05	1.575	2

After performing the tests and entering the response values in the software, the optimal model was selected. For data analysis, analysis of variance (ANOVA) was used. lack of fit data (Lack of fit), p value, F-value and R^2 were determined. In analysis of the results, F-value is an index to evaluate the significance of the model. The larger the numerical value, the more significant the model is, and p-value less than 0.05 is approved by model. The response variable was presented as a function of independent variables in the form of the polynomial regression model shown in Equation 3.

$$Y = b_0 + \sum_{i=1}^{n}(b_i X_i) + \sum_{i=1}^{n}\sum_{j=1}^{n}(b_{ij} X_i X_j) + \sum_{i=1}^{n}(b_{ii} X_i^2) \quad \text{(Eq. 3)}$$

In the above equation, Y is the response variable, b0 is the intercept, bi is the regression coefficient calculated from the values obtained from Y and Xi of the levels encoded by the independent variables, the XiXj and Xi2 parts comprise the interaction terms (interaction effect) and the quadratic effect, respectively.

2.6. Studies of the adsorption kinetics and isotherm

In order to study the kinetic behavior of dye adsorption on the proposed carbon composite, solutions with specific concentration of RR241 were prepared at pH = 5.0 and then 147 mg of GO-CC containing 4.15 wt. % of GO was added to them. At intervals of 5-120 min, the residual concentration of RR241 was measured (according to the procedure discussed before).

The equilibrium adsorption behavior of RR241 on the synthesized composite was also fitted to the Langmuir and Freundlich isotherms models. For this experiment, solutions with initial concentrations of 30, 50, 80, 100, 120, and 150 mg/L of the RR241 were prepared at pH = 5.0 and after adding 147 mg of the carbon composite containing 4.15 wt% of GO to them, the solutions were placed on a magnetic stirrer for 75 minutes (equilibrium time). The residual dye concentration in the solution was also determined using spectrophotometry. Langmuir and Freundlich isotherm models were used to analyze the data. The pseudo-first-order and pseudo-second-order kinetics were used to study the kinetics of the adsorption process. The rate constants of adsorption and the isotherms' constants were extracted to interpret the results, capacity, type, and energy of the adsorption process.

2.7. Structural characterization of the adsorbent

The morphology and surface porosity of the prepared carbon composites were studied using a Mira3 XMU model field emission scanning electron microscope (Tescan, Japan). Fourier transform infrared spectrometer (FTIR, Burker Alpha) was used to study the structural groups between composite and dye molecules. In this technique, the resolution of 2 cm-1 is used in the wavelength range of 4000-400 cm-1. The samples were completely powdered using KBr method and were prepared as discs by compression method. The textural properties of the prepared composite including porosity, average volume and pore size were explored with the aid of N2 adsorption/desorption isotherms using a Belsorp analyzer (BEL Japan Inc.) at 77 K. The specific surface area of the composites was also calculated using the Brunauer–Emmett–Teller (BET) method.

3. Results and Discussion

3.1. Characteristics of the suggested carbon composite as adsorbent

3.1.1. Morphology

FESEM images demonstrating the morphologies of the carbon composite before and after the modification with GO are shown in Fig 1 a-b, respectively. As shown in Figure 1, wrinkled GO sheets are present in the carbon composite (b), causing the surface area of the adsorbent, which interacts with the surrounding environment, especially, with the contaminant molecules in the solution, to be increased. This will be shown to be verified by examining the textural properties of both composites. This structure will be very effective in the process of adsorption of dyes from aqueous solutions.

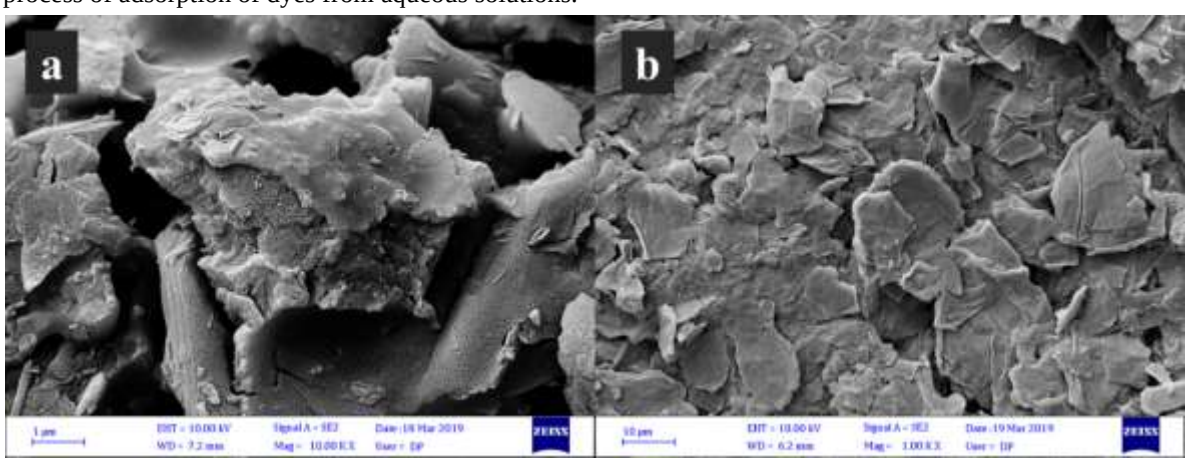

Figure 1. FESEM Images of the carbon composite a) before and b) after the modification with GO.

3.1.2. Potential at isoelectric point

The pH at the isoelectric point of an adsorbent is the point at which the number of positive and negative charges on the surface of the adsorbent are equal. In other words, the pH of the charge on the adsorbent surface is zero, referred to as the adsorbent isoelectric point or pHpzc. At pHs below pHpzc the adsorbent surface has a positive charge and at pHs above pHpzc the adsorbent has a negative charge. To determine this point, curve of the final pH of the solution containing the carbon composite is plotted against the initial pH of the solution, and the pHpzc is determined based on intersection of the curve with the line where final pH = initial pH, see

Figure 2. As shows the intersection point of the two plots is located at 5.7, indicating that the isoelectric point of the proposed adsorbent is 5.7, which is introduced as the potential at the isoelectric point.

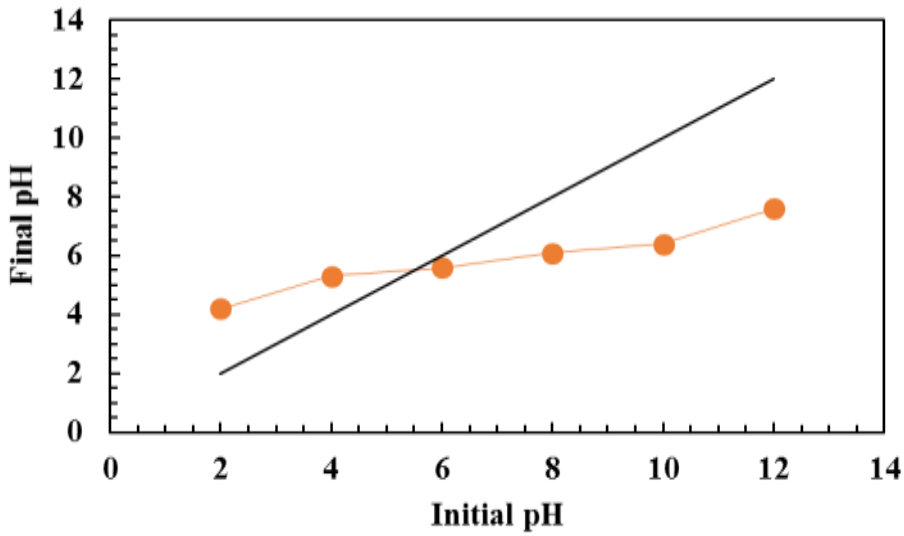

Figure 2. Diagram showing determination of potential at isoelectric point of the proposed adsorbent.

3.1.3. Textural characteristics

Textural characteristics including surface area, pore volume, and average pore size of GO-CC were determined by the BET method and were extracted from nitrogen adsorption-desorption isotherm diagrams (Fig. 3). For better comparison, the graphs of carbon composites without GO (CC) are also presented in the figure. The diagram shows that the presence of GO sheets in the carbon composite's structure amplifies the volumetric pressure of nitrogen gas adsorbed in the relative area of 0.7 to 0.9 with a steep upward slope compared to the unmodified sample. This sudden increase could be due to the capillary density inside the structure of GO-CC.

In addition, the calculations result of specific surface area, pore sizes, and average pore volume using BET are summarized in Table 2. The data in the table show that the texture characteristics of GO-CC are significantly higher than those (CC). The specific surface area and pore diameter of the GO-CC are 7.285 m2/g and 18.156 nm, respectively. However, the values for CC are 1.92 m2/g and 9.67 nm, respectively. The pore volume of GO-CC is about 2.5 times greater than CC. Increasing the pore volume and opening the pore diameter help improve the absorption efficiency of dye molecules on the nanocomposite surface and effectively remove them from aqueous solutions.

The results indicate that the integration of GO sheets with the activated carbon (graphite) and sol-gel process has caused the surface area, overall pore volume, and average composite pore size to be significantly increased. This may point out that the composite surface is more porous. In this way, it can be expected that the nano sheets can be easily separated from the solution by the formation of a porous and bulky composite through the stabilization of GO sheets in the composite matrix.

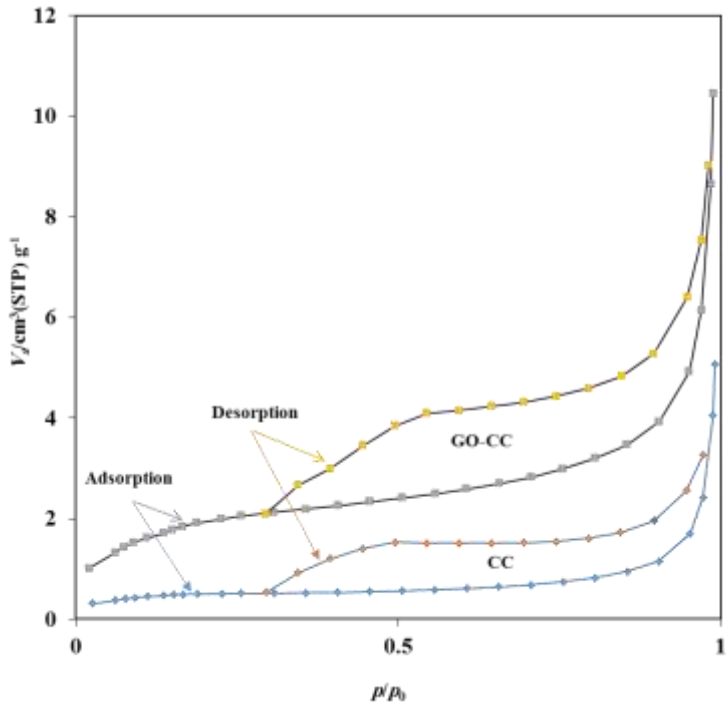

Figure 3. Nitrogen adsorption/desorption plot at 77.4 K for CC and GO-CC.

Table 2 Textural properties obtained by N_2 adsorption/desorption studies.

Parameters	Technique	CC	GO-CC
BET surface area (m2/g)	BET a	1.92	7.825
Pore volume (cm^3/g)	BJH adsorption [b]	0.007	0.017
Pore diameter (nm)	BJH adsorption	9.671	18.156

a Computed in the P/P_0 range of 0.05–0.50.
b BJH (Barrett Joyner Halenda) cumulative adsorption pore volume for pores having diameter in range of 0 and 50.0 Å.

3.1.4. FTIR Study

Figure 4 displays the FTIR spectra of GO-CC in the wavenumber range of the 4000-400 cm^{-1} before (curve A) and after absorption of RR241 (curve B), respectively. As can be seen, the functional groups present on GO-CC surface include OH groups with their characteristic absorption band at 3406 cm^{-1} and stretching of epoxy group (C–O–C) showing absorption peak at 1151 cm^{-1} [37,38].

In spectra B, which is related to the composite after contact with the dye, in addition to the characteristic peaks of the intact composite, new peaks have emerged that are likely correspond to RR241 functional groups. These peaks occurred at 1768 cm^{-1} belonging to stretching of C=O group, 1598 cm^{-1} for bending of N-H bond, 1498 cm^{-1} for stretching of N-O bond, 1417 cm^{-1} related to stretching of C-C bond in the aromatic ring, 1338 cm^{-1} for stretching of C-N and 771 cm^{-1} belonging to C-Cl group pertinent to the phenyl ring. The presence of

these peaks confirms the presence of azo dye on the surface of the carbon composite matrix after contact with the dye solution.

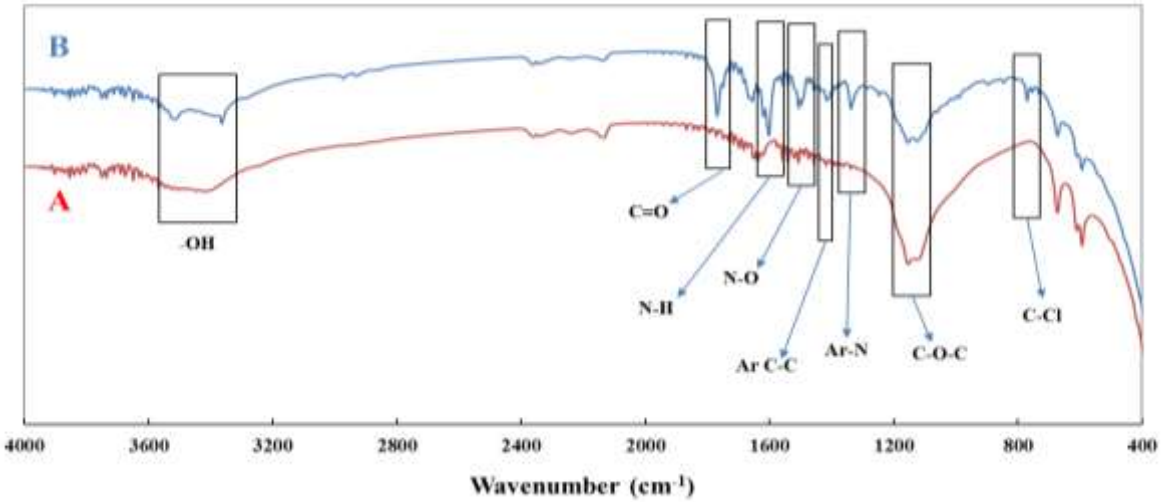

Figure 4. FTIR spectrums for GO-CC before (A) and After (B) adsorption of RR241.

3.2. Efficiency of GO-CC in RR241 dye removal

The efficiency of the GO-modified carbon composite in the removal of RR241 azo dye from its aqueous solutions was assessed by the central composite design route as a proper subset of RSM. The effects of pH, adsorption time, GO content in the composite and the adsorbent dose were investigated. The tests designed to optimize the removal conditions along with their responses are given in Table 3.

3.2.1. Statistical Findings

A quadratic model was achieved by prediction of the efficiency of RR241 removal using the response surface statistical method and Equation 6, which shows the empirical relationship between the selected variables and removal efficiency.

$$Re\ (\%) = -118.446 + 29.6\ X_1 + 1.09\ X_2 + 25.28\ X_3 + 50.91\ X_4 + 1.90\ X_3X_4 - 2.12X_1^2 - 4.37X_3^2 - 19.74X_4^2 \qquad (Eq.\ 6)$$

According to the results of the normal Probability of Internally Studentized Residuals (Figure 5), the model covers satisfactorily the ANOVA data. The residual values indicate the normal distribution of the operational variables near the mean values. Therefore, the regression model can be used to predict the removal efficiency of RR241 in the adsorption process. Figure 6 also shows the agreement between the experimental and the predicted values.

Table 3. Operational parameters and efficacy of dye removal after different runs.

Run	X_1: pH	X_2: Time (min)	X_3: GO content (%wt)	X_4: Adsorbent (GO-CC) (g/L)	Y: *Re* (%)
1	6.5	70	2.55	1.05	82.75
2	4.25	45	1.325	0.575	49.88
3	6.5	120	2.55	1.05	70.55
4	8.75	45	1.325	0.575	60.42
5	8.75	45	3.775	0.575	61.46
6	6.5	70	2.55	0.1	62.66
7	6.5	70	2.55	1.05	87.98
8	6.5	70	2.55	2	64.93
9	4.25	95	1.325	1.525	62.07
10	8.75	95	3.775	1.525	70.89
11	8.75	95	1.325	1.525	72.80
12	4.25	95	1.325	0.575	55.18
13	8.75	95	3.775	0.575	62.14
14	4.25	45	3.775	1.525	67.98
15	6.5	20	2.55	1.05	61.85
16	8.75	45	1.325	1.525	63.22
17	11	70	2.55	1.05	36.52
18	4.25	45	3.775	0.575	52.84
19	6.5	70	0.1	1.05	49.26
20	4.25	45	1.325	1.525	62.56
21	6.5	70	5	1.05	61.46
22	6.5	70	2.55	1.05	88.09
23	8.75	45	3.775	1.525	77.31
24	4.25	95	3.775	1.525	68.65
25	2	70	2.55	1.05	40.57
26	8.75	95	1.325	0.575	62.62
27	6.5	70	2.55	1.05	96.10
28	6.5	70	2.55	1.05	80.42
29	4.25	95	3.775	0.575	58.10
30	6.5	70	2.55	1.05	82.5

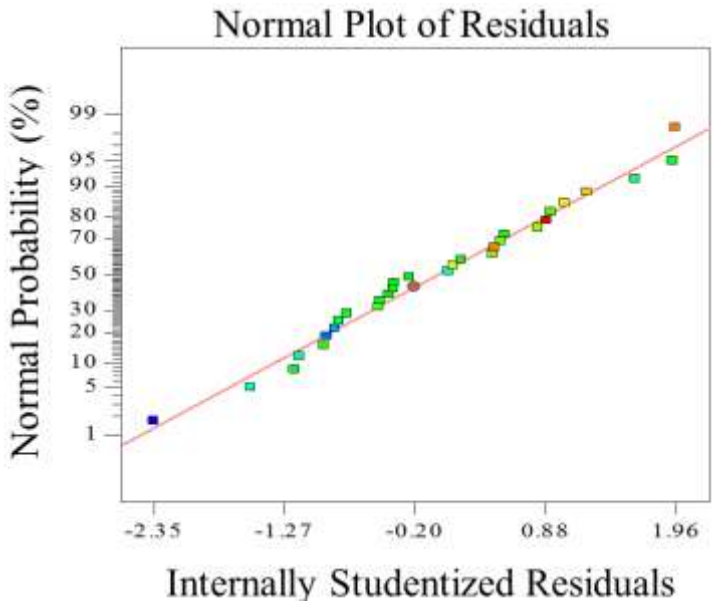

Figure 5. Normal probability distribution for residues of the RR241 removal by GO-CC.

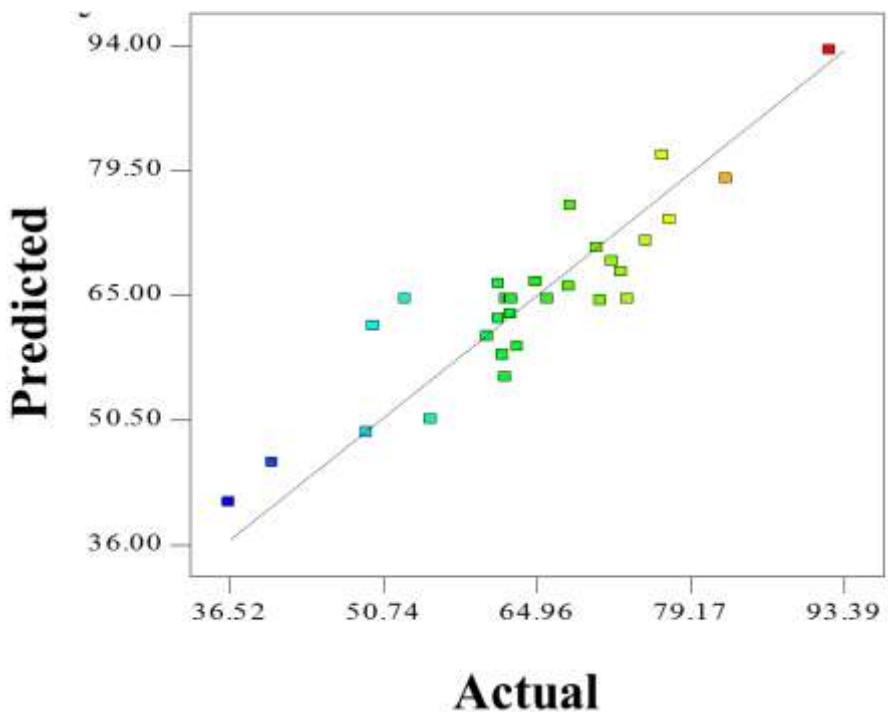

Figure 6. Relationship between experimental and predicted data (by RSM) of removal the RR241 using GO-CC.

The validity of the presented model was assessed by ANOVA (Table 4). Analysis of variance obtained from RSM for the adsorption process of RR241 by the proposed composite adsorbent shows that the parameters, pH (X_1), adsorption time (X_2), GO content in the composite (X_3), and the amount of adsorbent (X_4) as well as the interaction effect of pH and the adsorbent (X_1X_4), GO content and adsorbent (X_3X_4), X_1^2, X_3^2, and X_4^2 had significant effects on the removal efficiency.

The predicted R-value of 0.89 has reasonable conformity with the adjusted R^2 (0.932). Adeq adjusted measures noise, desirable values of which are more than 4. In this study, it was 9.61, which indicates a sufficient signal. Hence, this quadratic model can be used as a suitable spatial model for designing and optimizing the operational parameters.

Table 4. Analysis of variance of the data obtained from RSM for the adsorption process of RR241 dye by the composite adsorbent.

Source	Sum of Squares	df	Mean Square	F Value	p-value Prob > F	
Model	4725.29	14	337.52	5.098	< 0.0001	Significant
X1-pH	561.68	1	561.68	6.81	0.1980	
X2-time	524.12	1	524.12	6.02	0.3276	
X3-GO ratio	601.63	1	601.63	7.65	0.1241	
X4-absorbent	793.70	1	793.70	11.69	< 0.0001	
X1X2	476.83	1	476.83	5.29	0.8664	
X1X3	477.08	1	477.08	5.34	0.8548	
X1X4	479.14	1	479.14	5.77	0.7841	
X2X3	492.22	1	492.22	5.35	0.5612	
X2X4	481.81	1	481.81	5.13	0.7194	
X3X4	495.08	1	495.08	5.41	0.5300	
X1^2	3655.98	1	3655.98	71.89	< 0.0001	
X2^2	882.82	1	882.82	13.56	0.0104	
X3^2	1657.27	1	1657.27	29.85	< 0.0001	
X4^2	1019.69	1	1019.6	16.44	< 0.0001	
Residual	713.24	15	47.54			
Lack of Fit	549.4694	10	54.94694	1.67	0.2956	not significant
Pure Error	163.771	5	32.7542			
Cor Total	5438.536	29				

3.2.2. Effect of the variables on azo dye removal

The data presented in Table 4 and equation 4 indicate that amount of the carbon composite (X4) had the most effect on the removal process (coefficient of 50.91 and F value of 11.69) and adsorption time (X2) had the least effect compared to the other parameters (coefficient of 1.09 and F value of 6.02). The effects of independent variables on azo dye removal efficiency are illustrated in 3D plots of the response surface in Figure 7. In these diagrams, each factor except those involved in plots is fixed at a given value.

Figure 7a shows the effect of the amount of carbon composite as adsorbent, and pH of the solution on removal efficiency, while the time and GO content of the composite were assumed to be constant at 66 min and 4.0 wt%,

respectively. As the 3D plots show, the best efficiency was obtained at pH of 6.5 and the efficiency diminishes at a pH above and below it. The removal efficiency improves by increasing the amount of the composite adsorbent to the optimum amounts by increasing the amount of adsorbent from 0.1 g/L to 1.5 g /L, the removal efficiency amplifies from 30% to more than 80%.

The pH of solution is one of the contributing factors in the adsorption processes. Due to the presence of negative and positive species (OH^- and H^+) in the solution, pH changes can affect the adsorbent surface charge, the degree of ionization of various pollutants, the dissociation of functional groups on the active sites of the adsorbent and the structure of the dye molecule. Indeed, the solution pH affects the chemistry of the aquatic environment and the adsorbent surface groups.

The pHpzc of the adsorbent (GO-CC) was obtained to be 5.7 (see section 3.1.2); this means that the adsorbent surface is negatively charged at higher pH values, and at pH values below 5.7 the adsorbent surface charge is positive. Consequently, it is expected that at pH values below 5.7, the removal rate is upward, since in this range the opposite charges reach their maximum value and electrostatic attraction occurs between the adsorbent surface and dye molecules.

According to the findings of this study, amount of the carbon composite (or adsorbent dose) was the most contributing factor affecting removal efficiency. The effect of adsorbent mass is one of the most critical issues on the adsorption processes. According to the obtained results, removal efficiency improves with increasing adsorbent dose at constant concentration of RR241 dye. It can be stated that at a constant concentration of dye, as the adsorbent dose increases, the ratio of active sites present on the adsorbent surface to the number of RR241 molecules grows, resulting in enhancement of the removal efficiency. Whereas at low adsorbent amounts, the ratio of active sites to the adsorbed material molecules is low and consequently, the adsorption efficiency is little. But the interesting point is that by increasing the adsorbent dose beyond its optimum value, the adsorption capacity decreases from its maximum value. As the total number of active sites available at the adsorbent is proportional to the adsorbent dose, all active sites available on the adsorbent are not fully utilized in this condition, thus reducing the absorption capacity. This phenomenon can be attributed to the use of the available surface in the unsaturated form of the adsorbent.

The effects of time and the GO content of the carbon composite on the removal efficiency are shown in Figure 7b using a 3D graph of the response surface. As the graph shows, the removal efficieny increases with the elevation of GO content in the carbon composite matrix, so the removal efficiency increases from 30% to more than 78 % when the GO grows from 0.1 wt% to 3.8 wt%. If the GO content is kept in the same range and the time reaches 80 minutes, the removal efficiency is 84%.

An important issue when applying the adsorption system is to provide an effective contact time under certain conditions. However, in this study, based on the analysis of variance; time had the least effect on the proposed model.

For the concentration of 1.0 mM of the RR241, the adsorption process reaches equilibrium at 80 minutes and then exhibits a relatively constant trend. The effect of the contact time can be interpreted as the enhancement of the probability of collision of the contaminant molecules with the adsorbent surface by expansion of the contact time, and, as a result, the removal efficiency rises, and the amount of the dye residue in the solution diminishes.

Chemical properties as well as the high contact surface area (in other words, the surface-to-volume ratio) of GO has made this organic compound a suitable option for the removal of toxic, metallic species and pharmaceutical compounds. Ideally, GO has a completely two-dimensional structure, which is a monolayer nanostructure of carbon atoms bonded by covalent bonds, so that forms a perfectly flat honeycomb network [38]. In this carbon network, carbon atoms with hybridization of SP^2 form a two-dimensional plate with hydroxyl and epoxy groups being located on the carbon plate while carboxylic acid groups locating on the edges [40]. The presence of COOH and OH functional groups on GO sheet causes the contaminants to bond to the surface of the sheet by forming Van der Waals or electrostatic forces. However, in surface adsorption

applications, separation of the GO after the binding of the contaminants is difficult. In this study, two-dimensional GO sheets were incorporated into the carbon composite matrix through the sol-gel process, which allows it to be separated from the solution by filtration using Whatman 42D filter paper.

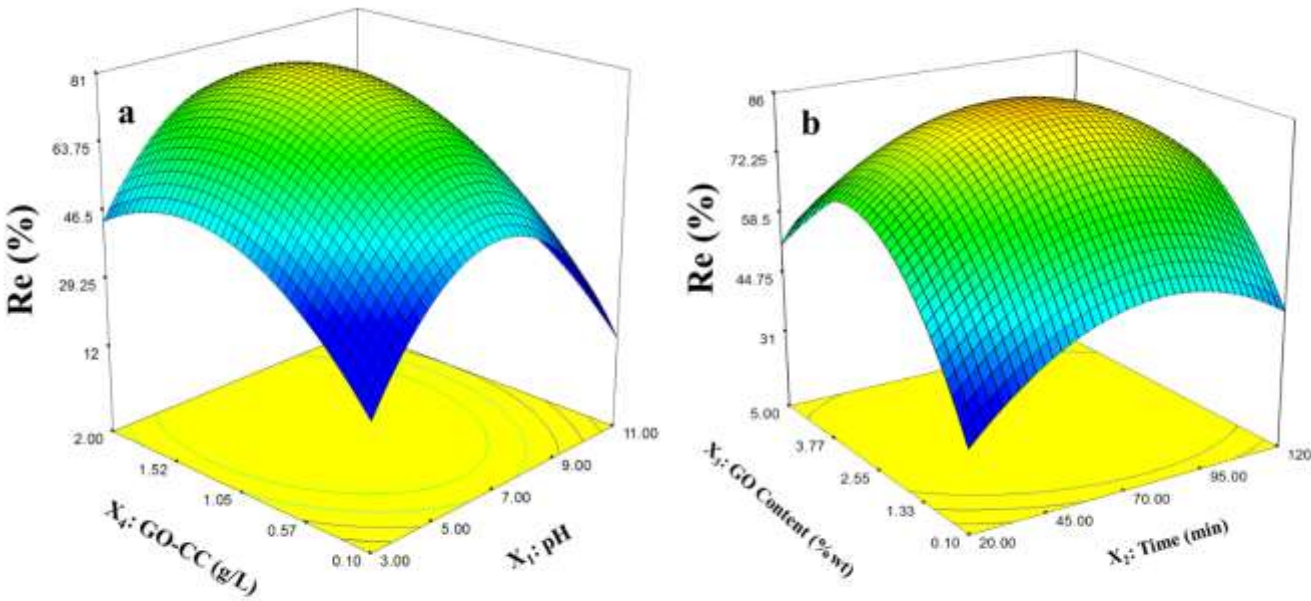

Figure 7- 3D surface plot for interaction effect of a) the pH and the adsorbent dose at constant adsorption time of 65 min and GO content of 4. 0 wt %. B) GO content and adsorption time at of pH 5.8 and adsorbent dose of 1.3 g/L.

Figure 7b shows that augmentation of GO content in the carbon composite improves the dye removal efficiency. This can be attributed to the increase in the available surface area, porosity, and the carbon composite pores due to the presence of GO, which was already mentioned in the study of the textural properties of the composite. Increment in the GO content can raise the pore diameter, increase the pore volume and improve the adsorbent surface area.

3.2.3 Optimization of the dye removal by GO-CC

The objective of optimization is to find a combination of variables that maximize removal. The RSM determines the best values for the process of variables, including pH, adsorption time, GO content and adsorbent dose. It is expected that this situation is considered as the best available conditions.

In DOE software, the desirability coefficient was chosen equal to 1 for maximum removal efficiency. As a result, 97% efficiency for RR241 removal was predicted by the model under optimal conditions as: pH of 5.0, adsorption time of 75 min, GO content of 4.15 wt. % and the adsorbent dose of 1.47 g/L.

3.3 Adsorption Kinetics

A study of the adsorption kinetics is suitable for the prediction of the adsorption rate and demonstration of the adsorption capacity over time and the type of adsorption mechanism. Hence, kinetic equations are used to describe the transfer behavior of the molecules adsorbed per unit time as well as to investigate the variables affecting the reaction rate. Two kinetic models of pseudo-first and second-order kinetic models were used to evaluate the kinetics of the dye adsorption. The pseudo-first-order kinetic model states that the diffusion process controls the reaction rate, while the pseudo-second-order kinetics states that the chemical absorption is the deceleration step of the reaction. Equations 7 and 8 give the pseudo-first-order and second-order kinetics, respectively:

$$\log(q_e - q_t) = \log q_e - \frac{k_1}{2.303} t \qquad \text{(Eq. 7)}$$

$$\frac{t}{q_t} = \frac{1}{k_2 q_e^2} + \frac{1}{q_e} t \qquad \text{(Eq. 8)}$$

In the above equations, q_e, q_t, k_1, and k_2 represent the equilibrium adsorption capacity (mg /g), the adsorption capacity (mg/g) at time t, the pseudo-first-rate constant, and the pseudo-second-order constant, respectively. Figure 8 shows the curves for the pseudo-first and second-order kinetics of RR241 adsorption. The obtained kinetic data are also summarized in Table 5.

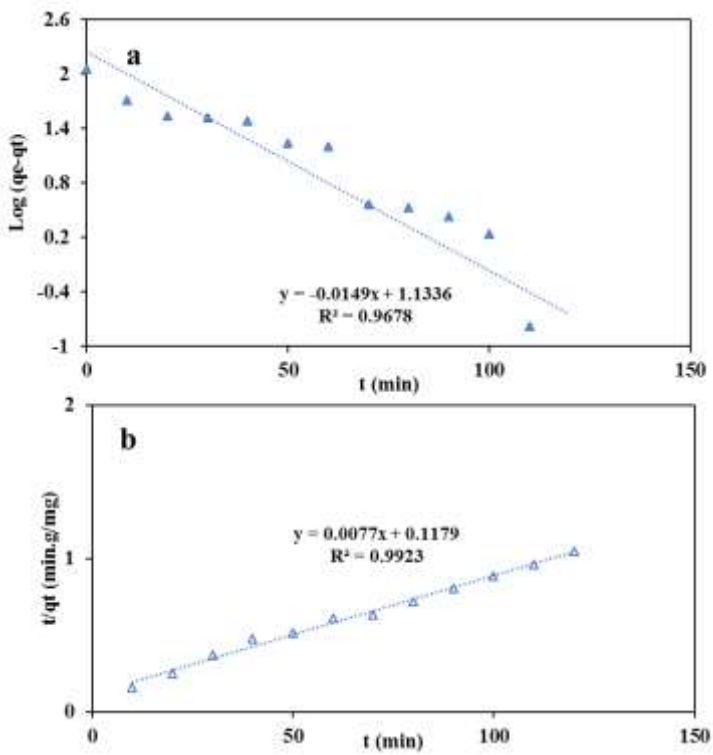

Figure 8. Kinetic plots for RR241 adsorption on GO-CC according to a) Pseudo-First-order and b) Pseudo-second-order models.

Table 5. Kinetic parameters for RR241 adsorption from aqueous using GO-CC at initial concentration of 100 mg/L.

Kinetic Model					
Pseudo-First-order			Pseudo-second-order		
K_1 (min^{-1})	q_e	R^2	K_2 (min^{-1})	q_e	R^2
0.034	21.67	0.9678	5.03	129.8	0.9923

A comparison of the coefficients shows that the pseudo-second-order kinetic model (R^2 = 0.9923) is more consistent and better suited to describe RR241 adsorption than the pseudo-first model (R^2 = 0.9678). The pseudo-second kinetics model shows that the adsorption rate is controlled by chemical bonding and the adsorption capacity is proportional to the active sites of the adsorbent [41]. In other words, the equation of the pseudo-second-order kinetics is chemical adsorption, and the adsorption process is slowed down because chemical adsorption is based on the adsorption of the solid phase. The pseudo-first-order kinetic equation is based on the adsorption capacity. If the adsorption process is restricted as a reversible process through the adsorbent boundary layer, the process follows the pseudo-first-order kinetic model. However, different mechanisms are involved in the adsorption process, including electrostatic and chemical interactions between active adsorption sites and pollutants [41]. The pseudo-first-order kinetic model indicates that the bonds depend on the reaction rate at concentrations or different pressures between the contaminant and the adsorbent surface. Wang et al. developed a GO doped with porous chitosan as an adsorbent to remove the methyl orange. The results showed that the adsorption process is well suited to pseudo-quadratic kinetics [42].

3.4 adsorption isotherm

Adsorption isotherms are equations to describe the equilibrium between the adsorbent and the pollutant. The most common models describing surface adsorption are the Langmuir and Freundlich models. The linear form of Freundlich and Langmuir isothermal models are expressed by Equations 9 and 10, respectively [43].

$$\ln q_e = \frac{1}{n}\ln C_e + \ln K_F \qquad \text{(Eq. 9)}$$

$$\frac{1}{q_e} = \frac{1}{C_e K_L q_m} + \frac{1}{q_m} \qquad \text{(Eq. 10)}$$

Where, q_e refers to amount of dye absorbed per unit mass of adsorbent at equilibrium (mg/g), C_e is dye equilibrium concentration (mg/L), K_F and n, reflect the intensity and capacity of adsorption, respectively. Also, in Langmuir equation, the q_m, adsorption capacity (mg/g), and b as the Langmuir constant represent the adsorption energy.

The isotherms diagram of Langmuir and Freundlich for the adsorption of RR241 using GO-CC is shown in Fig. 9. The values of the constants of Langmuir and Freundlich models with their correlation coefficients are presented in Table 7. Assessing the adsorption isotherms diagrams and comparison of correlation coefficients obtained from the two models express that the adsorption of RR241 on the modified carbon composite well fitted by the Langmuir model. Therefore, it can be said that the adsorption process of RR241 on the composite is monolayer and the maximum adsorption capacity is 160 mg/g.

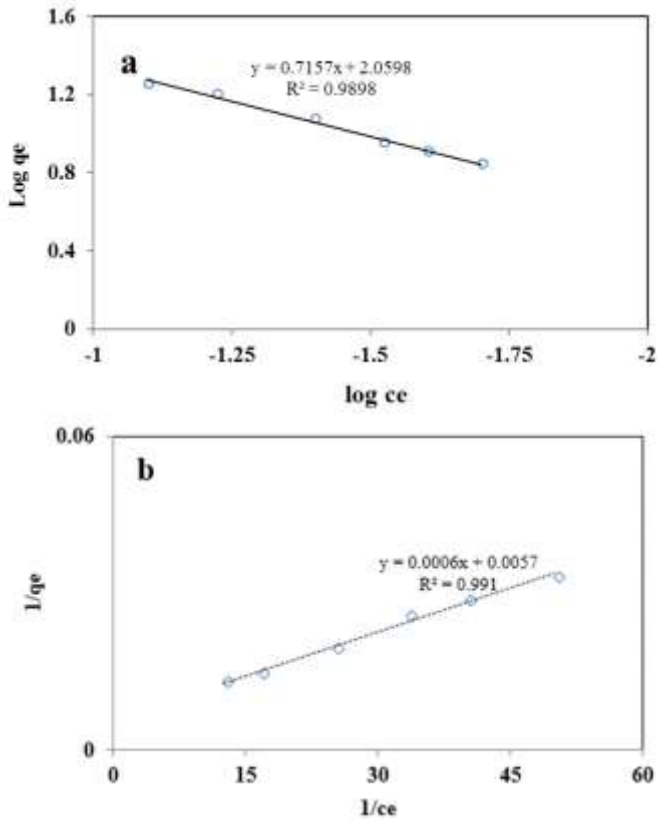

Figure 9. Fitting of RR241 adsorption on GO- carbon composite with a) Freundlich and b) Langmuir isotherm.

Table 7. Freundlich and Langmuir constants for adsorption of RR241 onto GO-CC.

Isotherm model	Parameters	
Freundlich	K_F	7.85
	$1/n$	0.716
	R^2	0.9898
Langmuir	q_{max}	160
	K_L	9.52
	R^2	0.991

In the Freundlich isotherm, as K_F increases, the adsorption capacity for the adsorbent for adsorbing the adsorbed material increases, and so n value between 1 and 10 represents the appropriate adsorption process. If the value of n is close to 1, the heterogeneity of the surface becomes less important and if it is close to 10, it becomes more important. The relevant parameters and coefficients are summarized in Table 7. In this study the

calculated value of K_F is 7.85, and the numerical value of n is 1.40, which is between the specified intervals. Therefore, the adsorption process of RR241 dye on the adsorbent is suitable.

3.5 Thermodynamics of the adsorption

Thermodynamic parameters comprising enthalpy change ($\Delta H°$), entropy change ($\Delta S°$), and Gibbs free energy change ($\Delta G°$) of RR241 adsorption are dependent on the coefficient of distribution of the adsorbed material between the solid and liquid phases. The thermodynamic parameters are expressed using Equations 11-13 [44-45]:

$$K_d = \frac{q_e}{C_e} \qquad \textit{(Eq. 11)}$$

$$\Delta G^0 = -RT\ Ln\ K_d \qquad \textit{(Eq. 12)}$$

$$Ln\ K_d = \left(\frac{\Delta S^0}{R}\right) - \left(\frac{\Delta H^0}{RT}\right) \qquad \textit{(Eq. 13)}$$

In these equations, K_d, R, and T are the distribution coefficients, the universal gas constant (8.314 J/molK), and the absolute temperature in K, respectively. The values of $\Delta H°$ and $\Delta S°$ are obtained from the slope and intercept of the linear plot of LnK_d versus 1/T.

The results of the effect of temperature on the removal process of RR241 are illustrated in Table 8 and Figure 10. The negative values of the ΔHº indicates that the adsorption process is exothermic and the dye removal rate decreases with increasing ambient temperature. The negative value of ΔGº also indicates the feasibility and spontaneity of the process. The negative ΔS^o values also indicate that the adsorption rate on the solid-liquid interface decrease during the adsorption process.

Table 8 - Thermodynamic parameters for the adsorption of RR241 by GO-CC.

C_e (ppm)	ΔH°	ΔS°	ΔG° (kJ/mol)			
	(kJ/mol)	(kJ/molK)	298	308	318	328
200	- 29.830	- 0.0736	-7.714	-7.047	-6.183	-5.073

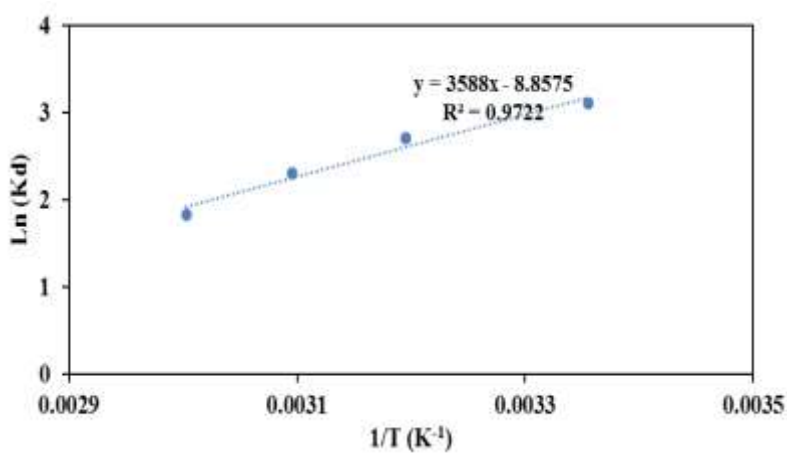

Figure 10. Thermodynamic Model of RR241 Adsorption on GO-CC.

4. Conclusion

The modified carbon composites with GO (GO-CC) were synthesized using sol-gel method. The structure and morphology properties of the prepared composites were investigated by BET, FTIR and SEM techniques. The prepared composites were used as an effective adsorbent for the removal of RR241 dye from aqueous solutions. The effect of different operational factors including pH, amount of GO in fabrication of the composite, amount of composite as adsorbent and the contact time were investigated by the response surface methodology. The removal experiments showed that the amount of the adsorbent, GO content and pH had a significant effect on RR241 removal. BET analysis indicated that the addition of GO to the carbon composite structure improved the pore size, total pore volume, and effective surface area of the composite. Also, isotherms, kinetics, and thermodynamic studies of adsorption were depicted that Langmuir isotherm model, pseudo-second-order kinetic model and self-adsorption are suitable models for RR241dye adsorption.

Acknowledgements

The authors would like to thank the Science and research Branch, Islamic Azad University; for the support of this research as well as the Nanobiotechnology Research Center in Yazd Branch, Islamic Azad University for providing their lab.

References

[1] Ma, B., Hauer, R. J., & Xu, C. (2020). Effects of design proportion and distribution of color in urban and suburban green space planning to visual aesthetics quality. Forests, 11(3), 278.
[2] Tamburini, D., Cartwright, C. R., Di Crescenzo, M. M., & Rayner, G. (2019). Scientific characterization of the dyes, pigments, fibres and wood used in the production of bark cloth from Pacific islands. Archaeological and Anthropological Sciences, 11(7), 3121-3141.
[3] Haji, A., & Naebe, M. (2020). Cleaner dyeing of textiles using plasma treatment and natural dyes: A review. Journal of Cleaner Production, 121866.
[4] Kabir, S. M. M., & Koh, J. (2018). Dyeing Chemicals. In Chemistry and Technology of Natural and Synthetic Dyes and Pigments. IntechOpen.
[5] Nambela, L., Haule, L. V., Mgani, Q. (2020). A review on source, chemistry, green synthesis and application of textile colorants. Journal of Cleaner Production, 246, 119036.
[6] Abdou, M. M. (2013). Thiophene-based azo dyes and their applications in dyes chemistry. American Journal of Chemistry, 3(5), 126-135.
[7] Ilyas, M., Ahmad, W., Khan, H., Yousaf, S., Yasir, M., & Khan, A. (2019). Environmental and health impacts of industrial wastewater effluents in Pakistan: a review. Reviews on environmental health, 34(2), 171-186.
[8] Colombetti, P., Calderon, M., Tello, J., González, P., & Jofré, M. (2020). Relationships between aquatic invertebrate assemblages and environmental quality on saline wetlands of an arid environment. Journal of Arid Environments, 181, 104245.
[9] Guadie, A., Yesigat, A., Gatew, S., Worku, A., Liu, W., Minale, M., & Wang, A. (2021). Effluent quality and reuse potential of urban wastewater treated with aerobic-anoxic system: A practical illustration for

environmental contamination and human health risk assessment. Journal of Water Process Engineering, 40, 101891.
[10] Lin J, Su T, Chen J, Xue T, Yang S, Guo P, Lin H, Wang H, Hong Y, Su Y, Peng L, Li J. Efficient adsorption removal of anionic dyes by an imidazolium-based mesoporous poly(ionic liquid) including the continuous column adsorption-desorption process, Chemosphere 2021; 272.
[11] Pai S, Kini MS, Selvaraj R. A review on adsorptive removal of dyes from wastewater by hydroxyapatite nanocomposites. Environ Sci Pollut Res 2021; 28: 11835–11849.
[12] Guo J, Yang Q, Meng QW, Lau C H, Ge Q. Membrane Surface Functionalization with Imidazole Derivatives to Benefit Dye Removal and Fouling Resistance in Forward Osmosis. ACS Appl Mater Interfaces 2021; 13 (5): 6710–6719.
[13] Moradihamedani P. Recent advances in dye removal from wastewater by membrane technology: a review. Polym Bull 2021.
[14] Mcyotto F, Wei Q, Macharia DK., Huang M, Shen C, Chow CWK. Effect of dye structure on color removal efficiency by coagulation. Chem Eng J 2021; 405: 126674.
[15] Bustos-Terrones Y A, Hermosillo-Nevárez JJ, Ramírez-Pereda B, Vaca M, Rangel-Peraza J G, Bustos-Terrones V, Rojas-Valencia MN. Removal of BB9 textile dye by biological, physical, chemical, and electrochemical treatments. J Taiwan Inst Chem E 2021; 121: 29-37.
[16] Kubra K T, Salman MSH, M Nazmul. Enhanced toxic dye removal from wastewater using biodegradable polymeric natural adsorbent. J Mol Liq 2021; 328: 115468
[17] Ata R and Tore GY. Characterization and removal of antibiotic residues by NFC-doped photocatalytic oxidation from domestic and industrial secondary treated wastewaters in Meric-Ergene Basin and reuse assessment for irrigation. J Environ Manage 233: 673-80 (2019).
[18] Kumari S, Khan AA, Chowdhury A, Bhakta AK, Mekhalif Z and Hussain S. Efficient and highly selective adsorption of cationic dyes and removal of ciprofloxacin antibiotic by surface modified nickel sulfide nanomaterials: Kinetics, isotherm and adsorption mechanism. Colloids Surf A Physicochem Eng Asp 586: 124264 (2020).
[19] Peng W, Li H, Liu Y and Song S. A review on heavy metal ions adsorption from water by graphene oxide and its composites. J Mol Liq 230: 496-504 (2017).
[20] Ahmad H, Fan M and Hui D. Graphene oxide incorporated functional materials: A review. Compos B Eng 145:270-280 (2018).
[21] Katsnelson MI. Graphene: carbon in two dimensions. Mater Today 10 (1–2): 20-27(2007).
[22] Cao G. Atomistic Studies of Mechanical Properties of Graphene. Polymers 6: 2404-2432 (2014).
[23] Sherlala AIA, Raman AAA, Bello MM and Asghar A. A review of the applications of organo-functionalized magnetic GO nanocomposites for heavy metal adsorption, Chemosphere 193: 1004-1017 (2018).
[24] Fraga TJ, Carvalho MN, Ghislandi MG and Motta Sobrinho MA. Functionalized graphene-based materials as innovative adsorbents of organic pollutants: A concise overview. Braz J Chem Eng 36(1): 1-31 (2019).
[25] Bhattacharyya A, Ghorai S, Rana D, Roy I, Sarkar G, Saha NR, Orasugh JT, De S, Sadhukhan S, Chattopadhyay D. Design of an efficient and selective adsorbent of cationic dye through activated carbon - graphene oxide nanocomposite: Study on mechanism and synergy. Mater Chem Phys 260: 1-10 (2021).
[26] Martins JT, Guimaraes CH, Silva PM, Oliveira RL, Prediger P. Enhanced removal of basic dye using carbon nitride/graphene oxide nanocomposites as adsorbents: high performance, recycling, and mechanism. Environ Sci Pollut Res 28, 3386–3405 (2021).
[27] Cao M, Shen Y, Yan Z, Wei Q, Jiao T, Shen Y, Han Y, Wang Y, Wang S, Xia Y, Yue T. Extraction-like removal of organic dyes from polluted water by the graphene oxide/PNIPAM composite system, Chem Eng J 405: 126647 (2021)
[28] Rostamian M, Hosseini H, Fakhri V, Yousefi Talouki P, Farahani M, Jalali Gharehtzpeh A, Goodarzi V, Su CH. Introducing a bio sorbent for removal of methylene blue dye based on flexible poly (glycerol sebacate)/chitosan/graphene oxide ecofriendly nanocomposites. Chemosphere 289:133219 (2022).

[29] Jafari S, Dehghani M, Nasirizadeh N and Azimzadeh M. An azithromycin electrochemical sensor based on an aniline MIP film electropolymerized on a gold nanourchins/graphene oxide modified glassy carbon electrode. J Electroanal Chem 829: 27-34 (2018).
[30] Aghili Z, Nasirizadeh N, Divsalar A, Shoeibi S and Yaghmaei P. A nanobiosensor composed of exfoliated graphene oxide and gold nano-urchins, for detection of GMO products. Biosens Bioelectron 95:72-80 (2017).
[31] Dehghani M, Nasirizadeh N and Yazdanshenas ME. Determination of cefixime using a novel electrochemical sensor produced with gold nanowires/graphene oxide/electropolymerized molecular imprinted polymer. Mater Sci Eng C 96:654-660 (2019).
[32] Seifati SM, Nasirizadeh N and Azimzadeh M. Nano-biosensor based on reduced graphene oxide and gold nanoparticles, for detection of phenylketonuria-associated DNA mutation. IET Nanobiotechnol. 12(4):417-422 (2017).
[33] Jafari S, Dehghani M, Nasirizadeh N, Baghersad MH and Azimzadeh M. Label-free electrochemical detection of Cloxacillin antibiotic in milk samples based on molecularly imprinted polymer and graphene oxide-gold nanocomposite. Measurement. 145:22-29 (2019).
[34] Rahman M, Cui D, Zhou S, Zhang A and Chen D. A GO coated gold nanostar based sensing platform for ultrasensitive electrochemical detection of circulating tumor DNA, Anal Methods 12 (2020) 440-447.
[35] Azimzadeh M, Nasirizadeh N, Rahaie M and Naderi-Manesh H. Early detection of Alzheimer's disease using a biosensor based on electrochemically-reduced graphene oxide and gold nanowires for the quantification of serum microRNA-137. RSC Adv 7(88):55709-55719 (2017).
[36] Wang Z, Pakoulev A, Pang Y and Dlott DD. Vibrational substructure in the OH stretching transition of water and HOD. J Physic Chem A 108(42):9054-9063 (2004).
[37] Hosseinzadeh M. sorption of lead ion from aqueous solution by carboxylic acid groups containing adsorbent polymer. J Chil Chem Soc 64(2): 4466-4470 (2019).
[38] Monji P, Jahanmardi R and Mehranpour M. Preparation of melamine-grafted graphene oxide and evaluation of its efficacy as a flame retardant additive for polypropylene. Carbon Lett 27:81-89 (2018).
[39] Sangster J. Octanol-water partition coefficients of simple organic compounds. J Phys Chem Ref Data 18(3): 1111-1229 (1989).
[40] Chavoshi N and Jahanmardi R. Chemical functionalization of graphene oxide by a hindered amine stabilizer and evaluation of the product as a UV-stabilizer for polypropylene. Fuller Nanotub Car N 27(1):1-9 (2019).
[41] Tabasideh S, Maleki A, Shahmoradi B, Ghahremani E and McKay G. Sonophotocatalytic degradation of diazinon in aqueous solution using iron-doped TiO2 nanoparticles. Sep Purif Technol 189:186-192 (2017).
[42] Wang Y, Xia G, Wu C, Sun J, Song R and Huang W. Porous chitosan doped with graphene oxide as highly effective adsorbent for methyl orange and amido black 10B. Carbohydr polym 115: 686-693 (2015).
[43] Esfandiyari T, Nasirizadeh N, Dehghani M and Ehrampoosh MH. Graphene oxide based carbon composite as adsorbent for Hg removal: Preparation, characterization, kinetics and isotherm studies. Chin J Chem Eng 25(9):1170-1175 (2017).
[44] Esfandiyari T, Nasirizadeh N, Ehrampoosh MH and Tabatabaee M. Characterization and absorption studies of cationic dye on multi walled carbon nanotube–carbon ceramic composite. J Ind Eng Chem 46:35-43 (2017).
[45] Boukhelkhal A, Benkortbi O and Hamadache M. Use of an anionic surfactant for the sorption of a binary mixture of antibiotics from aqueous solutions. Environ Technol 40(25): 3328-3336 (2019).